

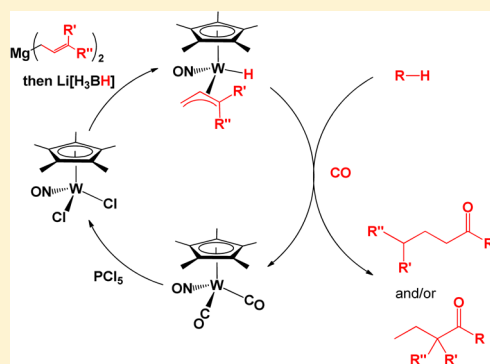
Unsymmetrical Saturated Ketones Resulting from Activations of Hydrocarbon C(sp³)-H and C(sp²)-H Bonds Effected by Cp*W(NO)(H)(η³-allyl) Complexes

Rhett A. Baillie, Guillaume P. Lefèvre, Russell J. Wakeham, Aaron S. Holmes, and Peter Legzdins*

Department of Chemistry, The University of British Columbia, Vancouver, British Columbia, Canada V6T 1Z1

S Supporting Information

ABSTRACT: C–H activations of a C(sp²)-H bond in benzene or a C(sp³)-H bond in mesitylene at 80 °C under CO pressure in undried solvents without rigorous exclusion of air and moisture can be effected with the 18e complexes Cp*W(NO)(H)(η³-CH₂CHCMe₂) (1), Cp*W(NO)(H)(η³-CH₂CHCHMe) (2), and Cp*W(NO)(H)(η³-CH₂CHCHPh) (3) (Cp* = η⁵-C₅Me₅). These activations are regioselective and afford in the case of complex 1 good yields of the unsymmetrical saturated ketones 4-methyl-1-phenylpentan-1-one (5) and 1-(3,5-dimethylphenyl)-5-methylhexan-2-one (8), respectively, in which the alkyl groups result from hydrogenation of the allyl ligand in the organometallic reactant. Complex 2 reacts similarly, but complex 3 only produces the ketone from its reaction with CO in benzene. Theoretical calculations indicate that the key mechanistic feature of these conversions is the formation of a 16e η²-alkene complex which is generated by the regioselective migration of the hydride ligand onto the tertiary carbon of the allyl ligand. The 16e Cp*W(NO)(η²-CH₂=CHCHMe₂) and Cp*W(NO)(η²-MeCH=CHPh) intermediate complexes formed in this manner by complexes 1 and 3, respectively, have been trapped as the corresponding 18e CO adducts Cp*W(NO)(CO)(η²-CH₂=CHCHMe₂) (10) and Cp*W(NO)(CO)(η²-MeCH=CHPh) (11). All new complexes have been characterized by conventional spectroscopic and analytical methods, and the solid-state molecular structures of two isomers of 11 have been established by single-crystal X-ray crystallographic analyses. This new and facile method of synthesizing saturated unsymmetrical ketones via C–C bond formation not only is atom economical but also is part of a complete synthetic cycle, since Cp*W(NO)(CO)₂ (4) is the final organometallic product formed in all cases, and it can be readily reconverted to the hydrido allyl reactants 1–3 in three steps via Cp*W(NO)Cl₂.



INTRODUCTION

The selective functionalization of C–H bonds continues to attract interest from synthetic, biological, and theoretical chemists, since recent advances in this field have begun to realize some of the early promise of this chemistry for the straightforward conversion of relatively simple substrates into more complex chemical entities.¹ Our recent contributions to this chemistry have involved the development of several 18e Cp*W(NO)(CH₂CMe₃)(η³-allyl) (Cp* = η⁵-C₅Me₅) compounds for the selective single activations of terminal C–H bonds of hydrocarbon substrates to produce isolable η¹-hydrocarbyl complexes.² The newly formed hydrocarbyl ligands in these latter compounds may then be functionalized and released by a variety of reagents.² We have now begun to extend our investigations to encompass the C–H activating abilities of the related 18e hydrido allyl complexes Cp*W(NO)(H)(η³-allyl)³ and in so doing have discovered some unprecedented chemistry effected by three of these compounds. Consequently, we now wish to report examples of the activations of hydrocarbon C(sp³)-H and C(sp²)-H bonds under CO pressure by Cp*W(NO)(H)(η³-CH₂CHCMe₂) (1), Cp*W(NO)(H)(η³-CH₂CHCHMe) (2), and Cp*W(NO)-

(H)(η³-CH₂CHCHPh) (3) that result in the liberation of unsymmetrical ketones via the formation of new C–C bonds.⁴

RESULTS AND DISCUSSION

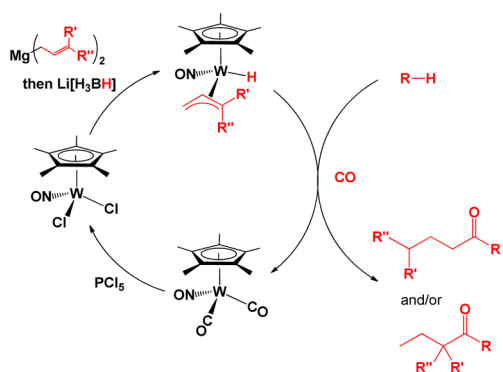
Chemical Conversions. The new chemistry that we have discovered is summarized in Scheme 1. It involves the synthesis of unsymmetrical saturated ketones via a C–H activation followed by the formation of two new C–C bonds.

The requisite 18e hydrido reagents 1–3 may be conveniently prepared in various isomeric forms from Cp*W(NO)Cl₂ by two sequential metathesis steps.³ In solution complex 1 exists as two coordination isomers in an 83/17 ratio, differing with respect to the endo/exo orientation of the allyl ligand. In contrast, complexes 2 and 3 each exist as four coordination isomers, all differing in the attachments of their allyl ligands, which can have either an endo or exo orientation with the methyl or phenyl groups being either proximal or distal to the nitrosyl ligand.³ All reactions of 1–3 have been performed with mixtures of these isomers, whose solution molecular structures

Received: June 19, 2015

Published: August 10, 2015

Scheme 1. Synthetic Cycle for Forming Unsymmetrical Saturated Ketones

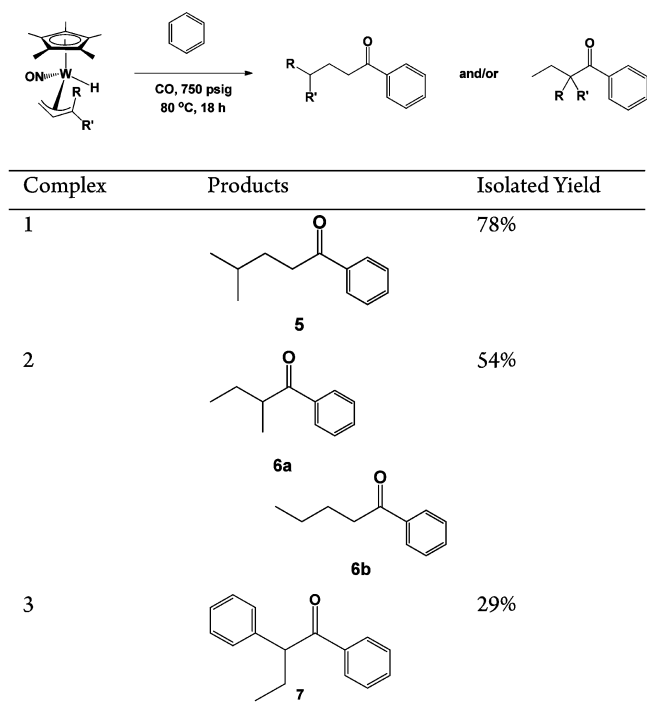


are consistent with the regioselective nature of the hydrocarbon–CO reaction depicted in Scheme 1 (vide infra).

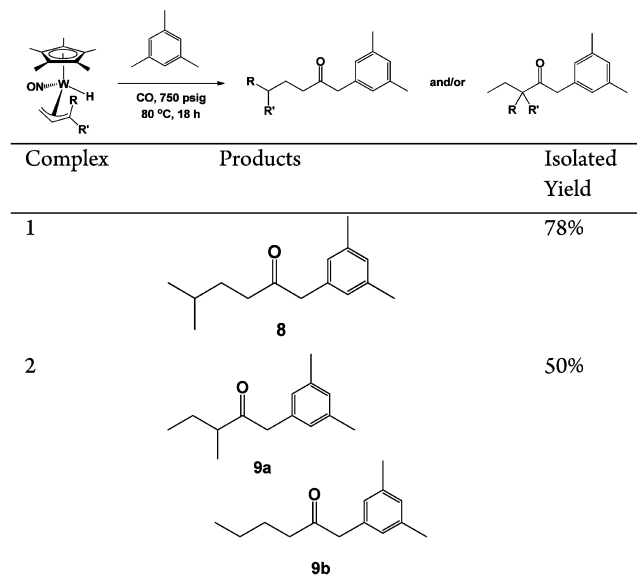
The formation of the unsymmetrical ketones shown in Scheme 1 involves one-pot C–H activation of the hydrocarbon followed by 1,1-CO insertion and coupling to the allyl ligand which has been hydrogenated by the hydride ligand and an H atom from the C–H activation. The organometallic final product in all cases is the well-known dicarbonyl nitrosyl complex $Cp^*W(NO)(CO)_2$ (4).⁵ Most notably, these conversions may be effected with undried solvents and without rigorous exclusion of moisture and air, since both the organometallic reactant and product are oxidatively and hydrolytically stable. To date benzene (Scheme 2) and mesitylene (Scheme 3) have been utilized as prototypical $C(sp^2)$ –H and $C(sp^3)$ –H bond containing R–H substrates to obtain the ketones indicated in unoptimized yields under the specified experimental conditions.

An interesting feature of the reactions presented in Scheme 1 is the degree of regioselectivity, particularly for the ketones

Scheme 2. Reactions Involving Benzene



Scheme 3. Reactions Involving Mesitylene



generated by complexes 1 and 3. Thus, the reaction of 1 with CO in benzene affords only a single ketone, 4-methyl-1-phenylpentan-1-one (5) (Scheme 2), a fact that can be explained by the solution isomers of 1, both of which have the methyl substituents of the allyl ligand proximal to the hydride ligand. The tertiary allyl carbon is the site of the allyl–hydride coupling, a feature that is reflected in the $CHMe_2$ terminus of the single organic product, 5. In contrast, the same reaction of 2 produces two ketones, 2-methyl-1-phenylbutan-1-one (6a) and 1-phenylpentan-1-one (6b) (Scheme 2). Again, the solution isomers of complex 2 are consistent with this result, since 2 exists as four isomers in solution with the methyl substituent of the allyl ligand being proximal to the hydride ligand for two isomers and proximal to the nitrosyl ligand for the other two isomers. These $Cp^*W(NO)(H)(\eta^3\text{-allyl})$ complexes also possess σ – π distorted allyl ligands, which result in their having unequal C–C bond lengths. The shorter C–C linkage with the greater sp^2 character C terminus is situated trans to the nitrosyl in each complex.³ It is this carbon that is the site of coupling with the hydride ligand.⁶ In other words, the substituents on the allyl ligand influence how it is coordinated to the metal center, and the σ – π distortion of the bound allyl ligand determines how it couples with the hydride ligand. These features are illustrated in Figure 1 to account for the production of the two ketones 6a,b, the higher yield of 6b

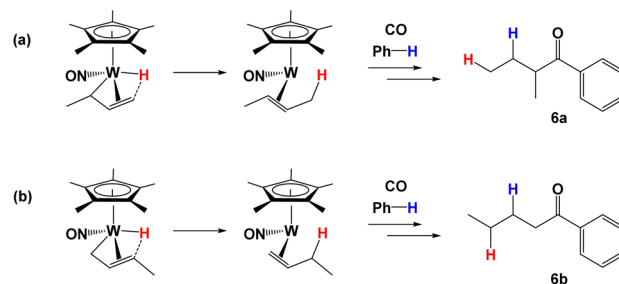


Figure 1. (a) Isomers of 2 with the methyl substituent of the allyl ligand proximal to the nitrosyl produce ketone 6a. (b) Isomers of 2 with the methyl substituent proximal to the hydride ligand produce ketone 6b.

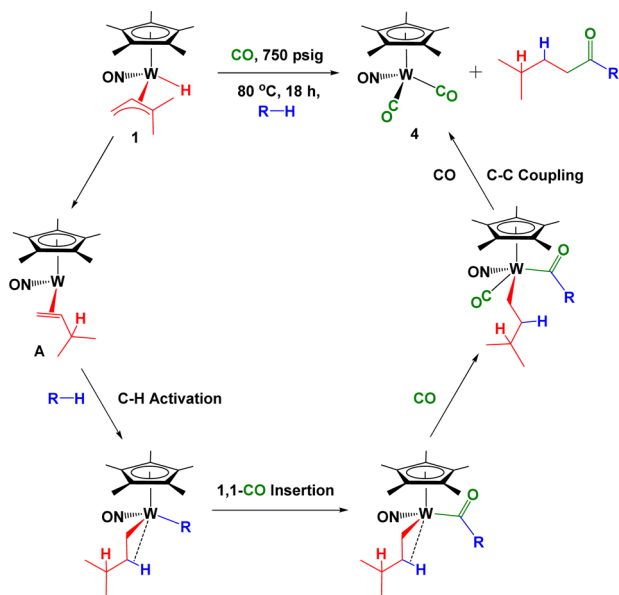
being reflective of the fact that principal isomers of **2** have the methyl group of the allyl ligand situated proximal to the hydride ligand.³

The reaction of **3** with CO in benzene produces a single ketone, **7** (Scheme 2), that does not follow the isomer trend observed for complexes **1** and **2**. This difference is probably an electronic effect due to the phenyl substituent on the allyl ligand. The two possible 16e η^2 -alkene intermediate complexes that **3** can generate contain either η^2 -MeCH=CHPh or η^2 -CH₂=CHCH₂Ph ligands. The reactive intermediate that contains the conjugated η^2 -*trans*- β -methylstyrene is likely favored on electronic grounds and is consistent with the formation of ketone **7**.

The reactions of **1** and **2** with CO in mesitylene (summarized in Scheme 3) parallel the reactions in benzene. Complex **1** gives a single organic product, namely 1-(3,5-dimethylphenyl)-5-methylhexan-2-one (**8**), while complex **2** affords the two ketones 1-(3,5-dimethylphenyl)-3-methylpentan-2-one (**9a**) and 1-(3,5-dimethylphenyl)-hexan-2-one (**9b**). These organic products are analogous to those formed by **1** and **2** with CO and benzene. The reaction of complex **3** with CO in mesitylene does not afford the expected ketone or any organic product. Instead, a single organometallic complex that sheds some light as to the mechanism operative during these conversions is produced (vide infra).

Mechanistic Considerations. The probable mechanism of the conversions involving benzene (Scheme 2) and mesitylene (Scheme 3) is outlined for complex **1** in Scheme 4, in which the organic reactants are represented by R–H for simplicity.

Scheme 4. Probable Mechanism of the Conversions Involving Complex 1

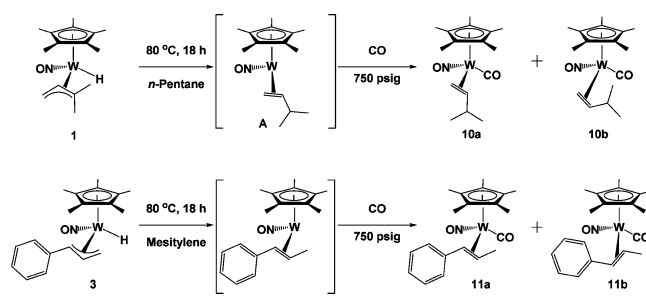


The key feature of the mechanism outlined in Scheme 4 is the formation of the 16e η^2 -alkene complex Cp*W(NO)(η^2 -CH₂=CHCHMe₂) (**A**), which is generated by a hydride shift to the tertiary carbon of the allyl ligand. This regioselective migration is consistent with the solution molecular structures established for both isomers of **1**, in which the two methyl substituents of the allyl ligand are proximal to the hydride.³ Furthermore, ketones such as CH₃CH₂CMe₂C(O)[CH₂(3,5-Me₂C₆H₃)] and Me₂CHCH(Me)C(O)[CH₂(3,5-Me₂C₆H₃)]

resulting from hydride migration to the other allyl carbons have not been detected in the final reaction mixtures. Further support for the existence of a 16e η^2 -alkene intermediate comes from the trapping of the Cp*W(NO)(η^2 -CH₂=CHCHMe₂) (**A**) and Cp*W(NO)(η^2 -MeCH=CHPh) intermediates formed by complexes **1** and **3**, respectively, by CO as the corresponding 18e adducts Cp*W(NO)(CO)(η^2 -CH₂=CHCHMe₂) (**10**) and Cp*W(NO)(CO)(η^2 -MeCH=CHPh) (**11**). These trapping reactions are described in the following paragraphs.

The reaction of **1** with CO in pentane does not afford a ketone resulting from pentane activation. Instead, the 18e CO adduct of the intermediate **A** can be isolated from the final reaction mixture (Scheme 5). Evidently **A** cannot effect the C–

Scheme 5. Trapping of Intermediate η^2 -Alkene Complexes with CO



H activation of pentane before reacting with CO. Adduct **10** exists as two isomers in a 52/48 ratio that have been characterized by 1D and 2D NMR spectroscopy, IR spectroscopy, and mass spectrometry. The η^2 coordination of the olefin ligand to the tungsten center is established by characteristic ¹⁸³W satellites evident in the ¹³C NMR spectrum (i.e., major isomer **10a**, δ 37.3 ppm (¹J_{WC} = 11.1 Hz, CH=CH₂), 59.2 ppm (¹J_{WC} = 38.8 Hz, CH=CH₂); minor isomer **10b**, δ 25.8 ppm (¹J_{WC} = 36.1 Hz, CH=CH₂), 65.2 ppm (¹J_{WC} = 9.9 Hz, CH=CH₂)). As shown in Scheme 5, the two isomers probably differ in the orientation of the CHMe₂ substituent on the bound olefin, as occurs for **11** (vide infra). The infrared nitrosyl stretching frequency for the mixture of isomers of **10** is 1614 cm⁻¹, the carbonyl stretching frequency is 1951 cm⁻¹, and the ¹³C NMR spectrum of **10** exhibits signals attributable to terminal carbonyls at δ 225.5 and 227.7 ppm for **10a,b**, respectively.

In contrast to complexes **1** and **2**, the reaction of **3** with CO in mesitylene does not lead to ketone formation but rather affords the trapped η^2 -alkene complex **11** (Scheme 5). As for the formation of **10** (vide supra), this outcome again reflects the kinetic discrimination between the two possible reaction pathways available to the η^2 -alkene intermediate complex. Complex **11** has been isolated as large orange plate crystals, and it exists as two isomers both in solution (**11a**, 63%; **11b**, 37%) and in the solid state (**11a**, 78%; **11b**, 22%) (Figures 2 and 3). The two isomers differ with respect to the orientation of the η^2 -*trans*- β -methylstyrene ligand. The phenyl substituent of the ligand is proximal to the nitrosyl ligand in both isomers, but the ligand differs in the *exo*/*endo* orientation of its substituents. The benzylic H is oriented proximal to the C₅Me₅ ligand in the major isomer (Figure 2) and distal in the minor isomer (Figure 3). This feature is also evident in the solution structures of the isomers, since the ¹H NMR spectrum of **11** confirms that the

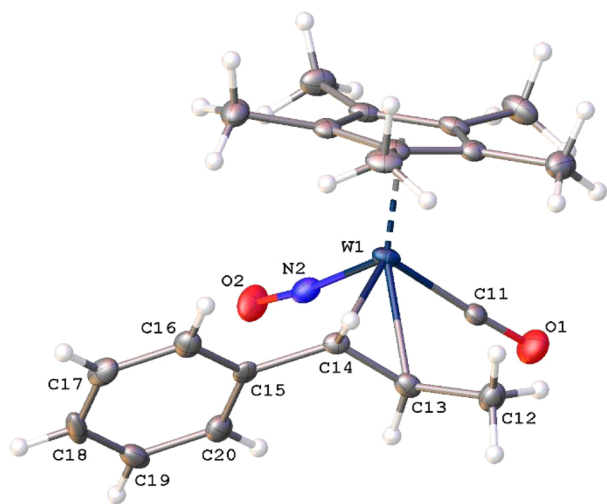


Figure 2. Solid-state molecular structure of **11a** with 50% probability thermal ellipsoids shown. Selected bond lengths (Å) and angles (deg): W(1)–N(1) = 1.826(4), N(2)–O(2) = 1.200(5), W(1)–C(11) = 1.925(5), C(11)–O(1) = 1.174(6), W(1)–C(13) = 2.288(6), W(1)–C(14) = 2.254(6), C(12)–C(13) = 1.513(7), C(13)–C(14) = 1.428(9), C(14)–C(15) = 1.498(6); W(1)–N(2)–O(2) = 173.1(4), W(1)–C(11)–O(1) = 177.1(4), C(12)–C(13)–C(14) = 122.3(5), C(13)–C(14)–C(15) = 125.4(5).

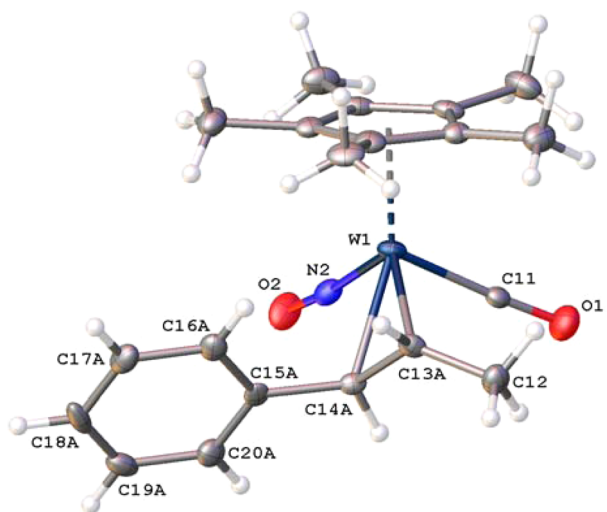


Figure 3. Solid-state molecular structure of **11b** with 50% probability thermal ellipsoids shown. Selected bond lengths (Å) and angles (deg): W(1)–C(13A) = 2.27(2), W(1)–C(14A) = 2.30(2), C(12)–C(13A) = 1.42(2), C(13A)–C(14A) = 1.40(3), C(14A)–C(15A) = 1.50(2); C(12)–C(13A)–C(14A) = 126(2), C(13A)–C(14A)–C(15A) = 128(2).

signal due to the benzylic H of **11a** has a greater upfield shift (δ 2.44 ppm) due to a stronger interaction with the tungsten center than does the signal for the benzylic H of **11b** (δ 4.06 ppm).³ The strong interaction between the tungsten center and the η^2 -alkene ligands is also evinced by the lengthened C=C bonds of 1.428(9) and 1.40(3) Å for **11a,b**, respectively. Consistently, the ¹³C NMR spectrum of **11** contains alkene C signals at δ 50.8 and 55.5 ppm for **11a** and δ 43.8 and 59.8 ppm for **11b**, significantly more upfield in comparison to those for a free alkene. The infrared stretching frequencies of the nitrosyl and carbonyl ligands are 1616 and 1956 cm⁻¹, and the ¹³C NMR signals for the carbonyl ligands of the isomers occur at δ

226.1 ppm for **11a** and δ 225.2 ppm for **11b**. These spectroscopic properties are very similar to those exhibited by the related complexes **10a,b**. Once formed, the CO adducts **10** and **11** are thermodynamically stable entities that evidently do not permit re-entry into the synthetic cycle under the experimental conditions employed (Scheme 1).

Theoretical Considerations. The results of DFT calculations on the transformation involving mesitylene and complex **1** (Scheme 3) are summarized in Figure 4 and corroborate the mechanistic proposals presented in Scheme 4. These calculations indicate that the first step is indeed the formation of the transient reactive 16e η^2 -alkene complex **A** (computed barrier 75.7 kJ mol⁻¹, TS₁). Complex **A** can then effect the C–H activation of one of the mesitylene C(sp³)–H bonds which also involves concerted migration of a hydrogen atom onto the ligated C=C double bond to lead to the bis(hydrocarbyl) 16e complex **B** with a barrier of 59.8 kJ mol⁻¹ (TS₂). Complex **B** is also stabilized by a β -agostic C–H interaction, as shown in Scheme 4. Coordination of a CO molecule onto the metal center in **B** affords complex **C**, and rapid migration (TS₃) of the mesityl group onto the W-ligated carbonyl group (computed barrier for the two steps 15.1 kJ mol⁻¹) results in the formation of complex **D** with a stabilization of 16.7 kJ mol⁻¹ with respect to complex **B**. Exothermic coordination of a CO molecule onto the metal in **D** can then take place, and complex **E** is thus obtained with a stabilization of 28.6 kJ mol⁻¹ with respect to **D**. Complex **E** then undergoes slow reductive coupling (75.9 kJ mol⁻¹, TS₄) to lead to the η^2 -CO ligated 3-methylbutyl mesityl ketone complex **F**. Further reaction with CO affords Cp*W(NO)(CO)₂ (**4**) and liberates the ketone **8** in an overall strongly exothermic process (overall stabilization of 232.9 kJ mol⁻¹ with respect to the reactants). This exothermicity leads to an overall nonreversible process which shifts all the preceding equilibria toward the formation of **8**. In other words, the theoretical calculations confirm that the overall conversion is very thermodynamically favored and that the rate-limiting steps are the formation of the η^2 -alkene complex **A** and the subsequent C–H activation of the hydrocarbon substrate by **A**. It is also worth noting at this point that the analogous Cp*W(NO)(CH₂CMe₃)(η^3 -allyl) complexes do not exhibit chemistry similar to that summarized in Scheme 1, presumably because upon thermolysis they form intermediate η^2 -diene and/or η^2 -allene complexes that effect the subsequent selective C–H activations.²

Concluding Comments. The syntheses of unsymmetrical saturated ketones have received considerable attention since they are reagents that are common to many organic transformations.⁷ For instance, a commonly employed method involves transition-metal-mediated syntheses (e.g., carbonylative Stille reactions), but these customarily employ costly metals such as palladium or toxic reagents such as alkyl tin compounds.⁸ In addition, reactive substrates such as carboxylic acid derivatives have also been utilized for this purpose,⁹ as has cross-coupling between pre-existing ketones.¹⁰ For example, a typical synthesis of unsymmetrical saturated ketones begins with the derivatization of a carboxylic acid to an acid chloride or an amide or direct treatment of the acid with an organometallic reagent (Scheme 6). However, these methods can pose significant complications due to the reactivity of the substrates and unwanted side reactions of the products.⁷

The new methodology for preparing such ketones described in this article complements existing synthetic methods. In addition, our new method of forming unsymmetrical ketones

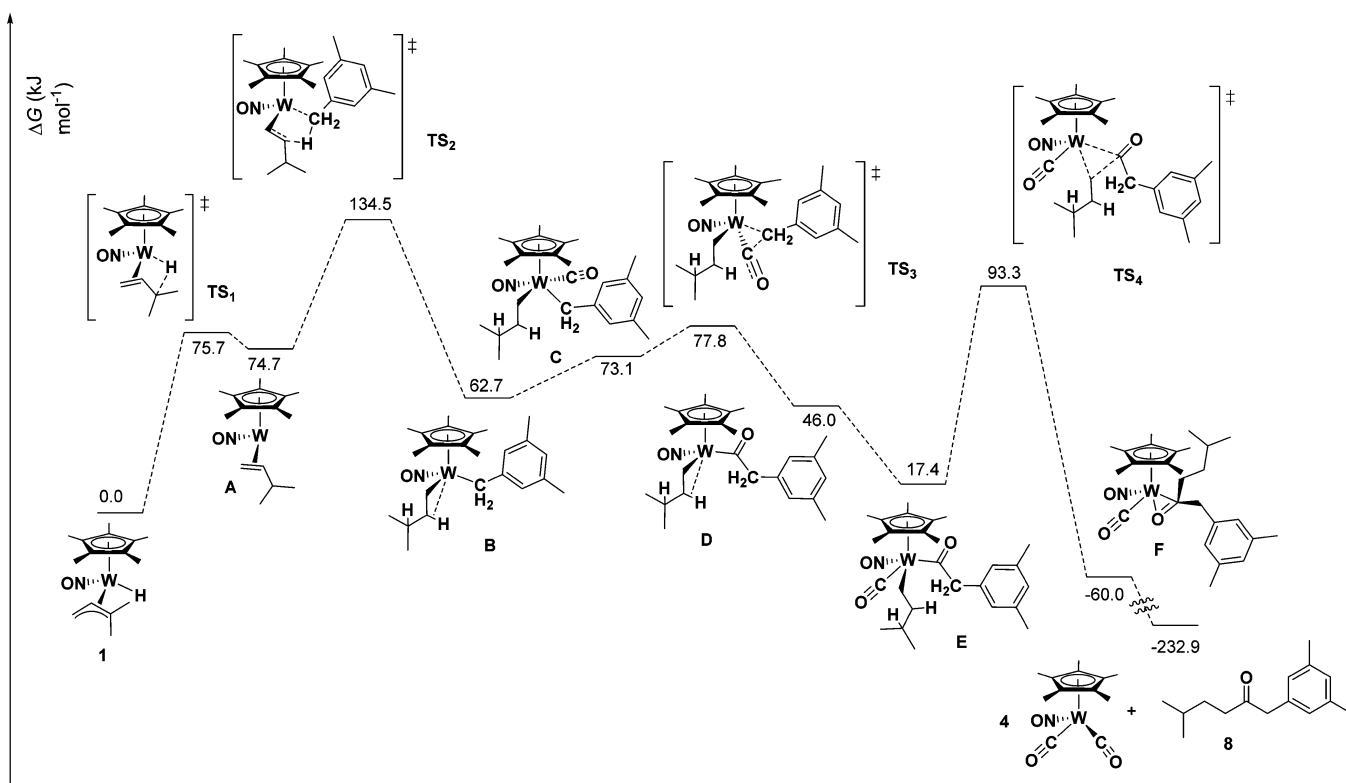
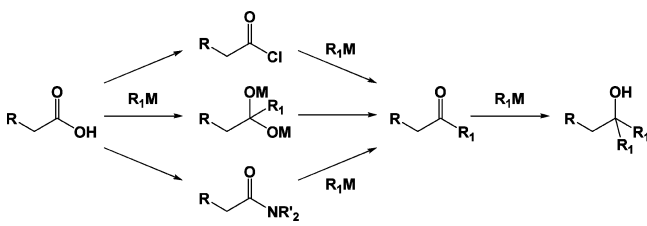


Figure 4. Computed ΔG values for the various species involved during the mesitylene reaction involving complex **1** shown in Scheme 3.

Scheme 6. Syntheses of Unsymmetrical Saturated Ketones



from unfunctionalized hydrocarbons and CO not only is atom economical but also, as indicated in Scheme 1, is part of a complete synthetic cycle, since the final organometallic product, namely $\text{Cp}^*\text{W}(\text{NO})(\text{CO})_2$, can be readily reconverted to the hydrido allyl reactant via $\text{Cp}^*\text{W}(\text{NO})\text{Cl}_2$, which is cleanly obtained by treatment of the dicarbonyl nitrosyl complex with PCl_5 .⁵

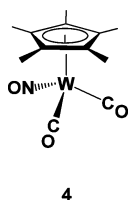
EXPERIMENTAL SECTION

General Methods. All reactions and subsequent manipulations involving organometallic reagents were performed under anhydrous and anaerobic conditions except where noted. All inert gases were purified by passing them through a column containing MnO and then through a column of activated 4 Å molecular sieves. High-vacuum and inert-atmosphere techniques were performed either using double-manifold Schlenk lines or in Innovative Technologies LabMaster 100 and MS-130 BG dual-station gloveboxes equipped with freezers maintained at -33°C . Preparative-scale reactions were performed with Schlenk or round-bottom flasks; reactions were performed in thick-walled glass reaction bombs (larger scale) or J. Young NMR tubes (smaller scale), both of which were sealed by Kontes greaseless stopcocks. Reactions with gases were performed in a Parr 5500 pressure reactor or a Parr 5500 pressure reactor modified with a sampling arm. If necessary, solvents were dried according to standard procedures.¹¹ The complexes $\text{Cp}^*\text{W}(\text{NO})(\text{H})(\eta^3\text{-CH}_2\text{CHCMe}_2)$ (**1**),

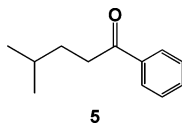
$\text{Cp}^*\text{W}(\text{NO})(\text{H})(\eta^3\text{-CH}_2\text{CHCHMe})$ (**2**), and $\text{Cp}^*\text{W}(\text{NO})(\text{H})(\eta^3\text{-CH}_2\text{CHCHPh})$ (**3**) were prepared according to the published procedures.³ Pentamethylcyclopentadiene was obtained from Boulder Scientific Co. All other chemicals and reagents were ordered from commercial suppliers and used as received.

Unless specified otherwise, all IR samples were prepared as Nujol mulls sandwiched between NaCl plates, and their spectra were recorded on a Thermo Nicolet Model 4700 FT-IR spectrometer. Except where noted, all NMR spectra were recorded at room temperature on Bruker AV-400 (direct and indirect probes) and AV-600 instruments, and all chemical shifts are reported in ppm and coupling constants are reported in Hz. ^1H NMR spectra were referenced to the residual protio isotopomer present in CDCl_3 (7.27 ppm) or C_6D_6 (7.16 ppm). ^{13}C NMR spectra were referenced to CDCl_3 (77.0 ppm) or C_6D_6 (128.39 ppm). For the characterization of the organometallic complexes, the two-dimensional NMR experiments $\{^1\text{H}-^1\text{H}\}$ COSY, $\{^1\text{H}-^{13}\text{C}\}$ HSQC, and $\{^1\text{H}-^{13}\text{C}\}$ HMBIC were performed to correlate and assign ^1H and ^{13}C NMR signals and establish atom connectivity. Low- and high-resolution mass spectra (EI, 70 eV) were recorded by Mr. Marshall Lapawa of the UBC mass spectrometry facility using a Kratos MS-50 spectrometer, and elemental analyses were performed by Mr. Derek Smith of the UBC microanalytical facility.

Reaction of 1 with Benzene and CO: Preparation of 4-Methyl-1-phenylpentan-1-one (5). In a glovebox, a Parr 5500 reactor was charged with **1** (0.300 g, 0.716 mmol) and dried benzene (ca. 75 mL), producing a yellow solution. The reactor was sealed, removed from the glovebox, and then purged three times with carbon monoxide. The reactor was pressurized to 750 psig of CO, and its contents were stirred and heated at 80°C for 18 h to produce an orange solution. The solvent was reduced in volume in vacuo to obtain a concentrated reaction mixture that was then purified by column chromatography on silica, the products being eluted independently using a gradient of 0–5% ethyl acetate in hexanes. The products of the reaction were identified as $\text{Cp}^*\text{W}(\text{NO})(\text{CO})_2$ (**4**; 14 mg, 5% yield) and **5** (98.2 mg, 78% yield).

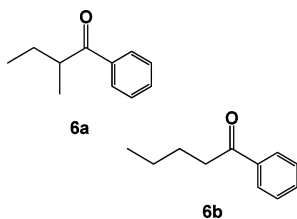


Characterization data for **4**, which agrees well with those previously reported:⁵ IR (cm⁻¹) 1993 (s, ν_{CO}), 1914 (s, ν_{CO}), 1655 (s, ν_{NO}); ¹H NMR (400 MHz, C₆D₆) δ 1.66 (s, 15H, C₅Me₅).



Characterization data for **5**, which agrees well with those previously reported:¹² IR (cm⁻¹) 1694 (s, ν_{CO}); MS (LREI, m/z , probe temperature 150 °C) 176 [M⁺]; ESI-MS theoretical m/z for [M + H]⁺ 177.1, found m/z for [M + H]⁺ = 177.2; MS (LREI, m/z , probe temperature 150 °C) 176 [M⁺], 105 [M⁺ - C₅H₁₁], 77 [M⁺ - C(=O)C₅H₁₁]; ¹H NMR (400 MHz, CDCl₃) δ 0.96 (d, ³J_{HH} = 5.8, 6H, Me), 1.619 (m, 2H, CH₂), 1.622 (m, 1H, CH), 2.97 (t, ³J_{HH} = 7.7, 2H, CH₂C(=O)), 7.46 (t, ³J_{HH} = 7.4, 2H, *m*-aryl H), 7.55 (t, ³J_{HH} = 7.4, 1H, *p*-aryl H), 7.97 (d, ³J_{HH} = 7.4, 2H, *o*-aryl H); ¹³C{¹H} NMR (100 MHz, CDCl₃) δ 22.4, 27.8, 33.2, 36.5, 128.0, 128.5, 132.8, 137.0, 200.6.

Reaction of 2 with Benzene and CO: Preparation of 2-Methyl-1-phenylbutan-1-one (6a) and 1-Phenylpentan-1-one (6b). In a glovebox, a Parr 5500 reactor was charged with **2** (0.159 g, 0.392 mmol) and dried benzene (ca. 30 mL), producing a dark yellow solution. The reactor was sealed, brought out of the glovebox, and then purged three times with carbon monoxide. The reactor was then pressurized to 750 psig of CO and was heated to 80 °C for 18 h while its contents were stirred. The reactor was then brought to room temperature and vented. The final reaction mixture was transferred to a round-bottom flask, and the solvent was removed in vacuo. The crude product was then purified via flash silica column chromatography with a gradient of 0–1% EtOAc in hexanes to give the organic products **6a** (0.017 g, 27%) and **6b** (0.017 g, 27%), as well as organometallic product **4** (<5% yield via NMR).

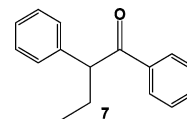


Characterization data for **6a**, which agrees well with those previously reported:¹³ IR (cm⁻¹) 1690 (s, ν_{CO}); MS (LREI, m/z , probe temperature 150 °C) 162 [M⁺]; ¹H NMR (400 MHz, CDCl₃) δ 0.91 (t, ³J_{HH} = 7.5, 3H), 1.19 (d, ³J_{HH} = 6.9, 3H), 1.45–1.56 (m, 1H), 1.78–1.90 (m, 1H), 3.40 (sext, ³J_{HH} = 6.7, 1H), 7.44–7.48 (m, 2H), 7.53–7.57 (m, 1H), 7.94–7.97 (m, 2H); ¹³C{¹H} NMR (100 MHz, CDCl₃) δ 11.9, 16.9, 26.6, 42.3, 128.4, 128.7, 132.9, 137.0, 204.6.

Characterization data for **6b**:¹⁴ ¹H NMR (400 MHz, CDCl₃) δ 0.95 (t, ³J_{HH} = 7.3, 3H), 1.41 (sext, ³J_{HH} = 7.6, 2H), 1.72 (quint, ³J_{HH} = 7.6, 2H), 2.97 (t, ³J_{HH} = 7.4, 2H), 7.44–7.48 (m, 2H), 7.53–7.57 (m, 1H), 7.94–7.97 (m, 2H); ¹³C{¹H} NMR (100 MHz, CDCl₃) δ 14.1, 22.6, 26.8, 38.5, 128.2, 128.7, 133.0, 137.3, 200.8.

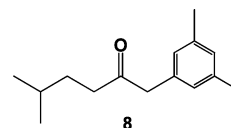
Reaction of 3 with Benzene and CO: Preparation of 1,2-Diphenylbutan-1-one (7). In a glovebox, a Parr pressure reactor was charged with **3** (0.200 g, 0.43 mmol) and benzene (ca. 20 mL). The pressure reactor was sealed and purged five times with carbon monoxide and finally pressurized to 750 psi. The reactor was connected to the mechanical stirrer, and its contents were heated to 80 °C while being stirred for 18 h. The reactor was cooled to room temperature, and the gas was carefully vented. The final reaction mixture was transferred to a round-bottom flask, and the volatiles were

removed in vacuo. The crude product was then purified by flash column chromatography on silica with a gradient 0–100% EtOAc in hexanes as eluent to give **7** as a yellow oil (0.0276 g, 29% yield).



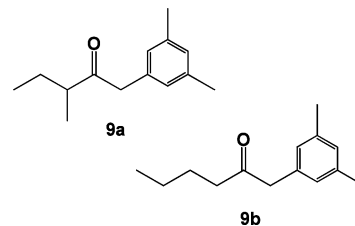
Characterization data for **7**, which agrees well with those previously reported:¹⁵ IR (cm⁻¹) 1694 (s, ν_{CO}); MS (LREI, m/z , probe temperature 150 °C) 224 [M⁺]; ¹H NMR (400 MHz, C₆D₆) δ 0.87 (t, ³J_{HH} = 7.4, 3H, Me), 1.75–1.89 (m, 1H, CH_aH_bCH₃), 2.09–2.25 (m, 1H, CH_aH_bCH₃), 4.40 (t, ³J_{HH} = 7.3, 1H, CH), 7.12–7.28 (m, 5H, Ar) 7.34 (t, ³J_{HH} = 7.6, 2H, *m*-aryl H), 7.44 (t, ³J_{HH} = 7.3, 1H, *p*-aryl H), 7.92 (d, ³J_{HH} = 7.2, 2H, *o*-aryl H); ¹³C APT NMR (100 MHz, C₆D₆) δ 12.4, 27.3, 55.6, 127.1, 128.4, 128.6, 128.8, 129.0, 132.9, 137.2, 139.8, 191.6.

Reaction of 1 with Mesitylene and CO: Preparation of 1-(3,5-Dimethylphenyl)-5-methylhexan-2-one (8). A Parr 5500 reactor was charged with **1** (0.300 g, 0.716 mmol) and mesitylene (ca. 20 mL). The reactor was sealed and purged with CO gas and finally pressurized to 750 psig of CO. The contents were heated to 80 °C while being stirred for 18 h. The reactor was then cooled, and the gas was carefully vented. The final dark red reaction mixture was collected, and the mesitylene was then removed by flash chromatography on silica using a gradient of 0–5% EtOAc in hexanes. The resulting crude product was further purified by column chromatography on silica using a gradient of 0–30% EtOAc in hexanes. The organic product **8** was obtained in good yield (122 mg, 78%). The organometallic product **4**⁵ was also isolated from the reaction mixture (33 mg, 11% yield), but much of it was lost with the mesitylene during the first separation.



Characterization data for **8**: IR (cm⁻¹) 1717 (s, ν_{CO}); MS (LREI, m/z , probe temperature 150 °C) 218 [M⁺]; ¹H NMR (400 MHz, CDCl₃) δ 0.85 (d, ³J_{HH} = 6.3, 6H, CHMe₂), 1.39–1.54 (m, overlapped, 1H, CHMe₂), 1.39–1.54 (m, overlapped, 2H, CH₂CHMe₂), 2.30 (s, 6H, ArMe₂), 2.44 (t, ³J_{HH} = 7.3, 2H, (C=O)CH₂CH₂CH), 3.61 (s, 2H, ArCH₂(C=O)CH₂), 6.82 (s, 2H, *o*-aryl H), 6.90 (s, 1H, *p*-aryl H); ¹³C NMR (100 MHz, CDCl₃) δ 22.5, 27.7, 32.7, 21.4, 40.1, 50.2, 125.6, 127.3, 128.7, 138.3, 209.2.

Reaction of 2 with Mesitylene and CO: Preparation of 1-(3,5-Dimethylphenyl)-3-methylpentan-2-one (9a) and 1-(3,5-Dimethylphenyl)hexan-2-one (9b). In a glovebox, a Parr 5500 reactor was charged with **2** (0.290 g, 0.716 mmol) and dried mesitylene (ca. 15 mL), producing a dark yellow solution. The reactor was sealed and was then purged three times with carbon monoxide. The reactor was finally pressurized to 750 psig of CO, and the contents were stirred while being heated to 80 °C for 18 h. The reactor was then cooled to room temperature and vented carefully. The dark brown crude product was then purified via flash silica column chromatography with a gradient of 0–5% EtOAc in hexanes to give the two novel organic products **9a** (0.0109 g, 7% yield) and **9b** (0.0632 g, 43% yield) as a yellow oil, as well as the organometallic product **4** (0.044 g, 15% yield).

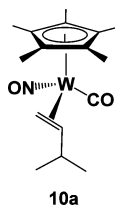


Characterization data for **9a**: IR (cm⁻¹) 1716 (s, ν_{CO}); MS (LREI, m/z , probe temperature 150 °C) 204 [M⁺]; MS (HREI-MS, m/z) calcd for C₁₄H₂₀O 204.15142, found 204.15154; ¹H NMR (400 MHz,

CDCl_3) δ 0.84 (t, $^3J_{\text{HH}} = 7.5$, 3H, CH_3), 1.06 (d, $^3J_{\text{HH}} = 6.9$, 3H CH_3), 1.39 (quint, $^3J_{\text{HH}} = 7.0$, 2H, CH_2), 2.29 (s, 6H, ArMe_2), 2.58 (sext, $^3J_{\text{HH}} = 6.8$, 1H, CH), 3.64 (s, 2H, CH_2), 6.81 (s, 2H, *o*-aryl H), 6.89 (s, 1H, *p*-aryl H); ^{13}C NMR (100 MHz, CDCl_3) δ 11.7, 16.2, 21.4, 26.1, 47.0, 48.6, 127.4, 128.6, 134.2, 138.2, 212.3.

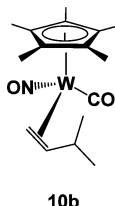
Characterization data for **9b**: ^1H NMR (400 MHz, CDCl_3) δ 0.87 (t, $^3J_{\text{HH}} = 7.3$, 3H, CH_3), 1.26–1.29 (overlapped, CH_2), 1.53 (quint, $^3J_{\text{HH}} = 7.5$, 2H, CH_2), 2.29 (s, 6H, ArMe_2), 2.43 (t, $^3J_{\text{HH}} = 7.3$, 2H, CH_2), 3.59 (s, 2H, CH_2), 6.81 (s, 2H, *o*-aryl H), 6.89 (s, 1H, *p*-aryl H); ^{13}C NMR (100 MHz, CDCl_3) 13.9, 21.4, 22.4, 26.0, 41.8, 50.2, 127.3, 128.7, 134.4, 138.3, 209.1.

Preparation of Cp*W(NO)(CO)(η^2 - $\text{CH}_2=\text{CHCHMe}_2$) (10). A Parr 5500 reactor was charged with **1** (0.200 g, 0.477 mmol) and *n*-pentane (ca. 100 mL). The reactor was sealed and purged with CO gas and finally pressurized to 750 psig of CO. The contents were heated to 80 °C while being stirred for 18 h. The reactor was then cooled to room temperature, and the gas was carefully vented. The final orange reaction mixture was collected, and the solvent was removed in vacuo to give a dark orange oily residue. The crude product was purified via flash column chromatography on silica with a gradient 0–100% EtOAc in hexanes as eluent. Two isomers of **10** were isolated as an orange solid (28 mg, 13% yield).



10a

Characterization data for **10a** (52%): IR (cm^{-1}) 1951 (s, ν_{CO}) 1614 (s, ν_{NO}); MS (LREI, m/z , probe temperature 150 °C) 447 [M^+ , ^{184}W], 419 [$\text{M}^+ - \text{CO}$, ^{184}W], 417 [$\text{M}^+ - \text{NO}$, ^{184}W]; ^1H NMR (600 MHz, C_6D_6) δ 0.898 (obscured, 1H, $\text{CH}=\text{CH}_2$), 1.24 (d, $^3J_{\text{HH}} = 6.3$, 3H, CHMe_2), 1.29 (d, $^3J_{\text{HH}} = 6.3$, 3H, CHMe_2), 1.60 (s, 15H, C_5Me_5), 1.65 (obscured, 1H, CHMe_2), 1.68 (m, 1H, $\text{CH}=\text{CH}_2$), 2.43 (dd, $^3J_{\text{HH}} = 9.8$, $^2J_{\text{HH}} = 4.4$, 1H, $\text{CH}=\text{CH}_2$); ^{13}C APT NMR (150 MHz, C_6D_6) δ 10.3 (C_5Me_5), 24.4 (CHMe_2), 30.1 (CHMe_2), 37.3 (s, $^1J_{\text{WC}} = 11.1$, $\text{CH}=\text{CH}_2$), 38.6 (CHMe_2), 59.2 (s, $^1J_{\text{WC}} = 38.8$, $\text{CH}=\text{CH}_2$), 104.52 (C_5Me_5), 225.5 (W–CO).

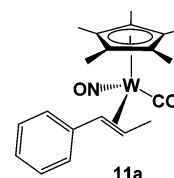


10b

Characterization data for **10b** (48%): ^1H NMR (600 MHz, C_6D_6) δ 0.88 (m, 1H, $\text{CH}=\text{CH}_2$), 0.900 (d, $^3J_{\text{HH}} = 6.8$, 3H, CHMe_2), 1.39 (d, $^3J_{\text{HH}} = 6.6$, 3H, CHMe_2), 1.60 (s, 15H, C_5Me_5), 1.969 (m, 1H, $\text{CH}=\text{CH}_2$), 1.973 (m, 1H, $\text{CH}=\text{CH}_2$), 2.90 (m, 1H, CHMe_2); ^{13}C APT NMR (150 MHz, C_6D_6) δ 10.4 (C_5Me_5), 20.5 (CHMe_2), 25.8 (s, $^1J_{\text{WC}} = 36.1$, $\text{CH}=\text{CH}_2$), 28.9 (CHMe_2), 33.6 (CHMe_2), 65.2 (s, $^1J_{\text{WC}} = 9.9$, $\text{CH}=\text{CH}_2$), 104.54 (C_5Me_5), 227.7 (W–CO).

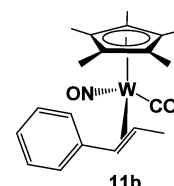
Preparation of Cp*W(NO)(CO)(η^2 -MeCH=CHPh) (11). In a glovebox, a Parr pressure reactor was charged with **3** (0.200 g, 0.43 mmol) and mesitylene (ca. 20 mL). The pressure reactor was sealed and purged five times with carbon monoxide before being finally pressurized to 750 psig. The reactor was connected to the mechanical stirrer, and its contents were heated to 80 °C while being stirred for 18 h. The reactor was cooled to room temperature, and the gas was carefully vented. The final reaction mixture was transferred to a round-bottom flask, and the volatiles were removed in vacuo. The crude product was then purified by flash column chromatography on silica with a gradient 0–100% EtOAc in hexanes as eluent to give two isomers of Cp*W(NO)(CO)(η^2 -MeCH=CHPh) (**11**) as an orange solid (0.0222 g, 19% yield). Crystals of **11** suitable for a single-crystal

X-ray diffraction analysis were grown by layering CH_2Cl_2 /hexanes at room temperature in the air.



11a

Characterization data for **11a** (63%): IR (cm^{-1}) 1616 (s, ν_{NO}), 1955 (s, ν_{CO}); MS (LREI-MS, m/z , probe temperature 150 °C) 495 [M^+ , ^{184}W]; MS (HREI-MS, m/z , ^{182}W) calcd for $\text{C}_{20}\text{H}_{25}\text{NO}^{182}\text{W}$ 493.13675, found 493.13717; ^1H NMR (400 MHz, C_6D_6) δ 1.57 (d, $^3J_{\text{HH}} = 6.5$, 3H, CHCH_3), 1.59 (s, 15H, C_5Me_5), 2.44 (d, $^3J_{\text{HH}} = 10.5$, 1H, PhCHCHCH_3), 3.52 (dq, $^3J_{\text{HH}} = 10.5$, 6.5, 1H, PhCHCHCH_3), 6.94 (t, $^3J_{\text{HH}} = 7.3$, 1H, *p*-aryl H), 7.03 (d, $^3J_{\text{HH}} = 7.3$, 2H, *o*-aryl H) 7.26 (t, $^3J_{\text{HH}} = 7.8$, 2H, *m*-aryl H); ^{13}C APT NMR (100 MHz, C_6D_6) δ 10.2 (C_5Me_5), 21.4 (PhCHCHCH_3), 50.8 (PhCHCHCH_3), 55.5 (PhCHCHCH_3), 105.1 (C_5Me_5), 124.6 (*p*-aryl C), 125.4 (*o*-aryl C), 128.1 (*m*-aryl C), 147.0 (*i*-aryl C), 226.1 (W–CO). Anal. Calcd for $\text{C}_{20}\text{H}_{25}\text{NOW}$: C, 48.50; H, 5.09; N, 2.83. Found: C, 48.47; H, 5.08; N, 2.83.



11b

Characterization data for **11b** (37%): ^1H NMR (400 MHz, C_6D_6) δ 1.54 (s, 15H, C_5Me_5), 2.15 (d, $^3J_{\text{HH}} = 5.8$, 3H, CHCH_3), 2.29–2.35 (m, 1H, PhCHCHCH_3), 4.06 (d, $^3J_{\text{HH}} = 11.1$, 1H, PhCHCHCH_3), 6.88 (t, $^3J_{\text{HH}} = 7.1$, 1H, *p*-aryl H), 6.99 (d, $^3J_{\text{HH}} = 7.6$, 2H, *o*-aryl H) 7.10 (t, $^3J_{\text{HH}} = 7.7$, 2H, *m*-aryl H); ^{13}C APT NMR (100 MHz, C_6D_6) δ 10.0 (C_5Me_5), 24.1 (PhCHCHCH_3), 43.8 (PhCHCHCH_3), 59.8 (PhCHCHCH_3), 104.8 (C_5Me_5), 125.2 (*p*-aryl C), 125.8 (*o*-aryl C), 128.0 (*m*-aryl C), 143.9 (*i*-aryl C), 225.2 (W–CO).

X-ray Crystallography. Data collection was carried out at -173.0 ± 2 °C on a Bruker X8 APEX II diffractometer with graphite-monochromated Mo $K\alpha$ radiation.

Data for **11** were collected to a maximum 2θ value of 55.078° in 0.5° oscillations with 3.0 s exposures. The structure was solved by direct methods¹⁶ and expanded using Fourier techniques. The C12–C20 fragment was disordered in two orientations with a 0.782(6):0.218(6) occupancy ratio. All non-hydrogen atoms were refined anisotropically, and hydrogen atoms were placed in calculated positions. The final cycle of full-matrix least-squares analysis was based on 4227 observed reflections and 223 variable parameters.

Neutral-atom scattering factors were taken from Cromer and Waber.¹⁷ Anomalous dispersion effects were included in F_o ;¹⁸ the values for $\Delta f'$ and $\Delta f''$ were those of Creagh and McAuley.¹⁹ The values for mass attenuation coefficients were those of Creagh and Hubbell.²⁰ All refinements were performed using SHELXL-2014²¹ via the OLEX2 interface.²² X-ray crystallographic data for the structure are presented in Table S1 in the Supporting Information, as are full details of the crystallographic analysis.

Computational Methods. Density functional theory²³ was applied to determine the structural and energetic features of the various organometallic complexes described in this article. All theoretical calculations were performed using Gaussian 09.²⁴ The 6-31+G(d) basis set^{25,26} was used for all atoms (C, H, O, N) except W, which was treated using the Stuttgart pseudopotential and associated basis set.²⁷ The hybrid exchange correlation functional PBE0 was also used.²⁸ It mixes 25% of Hartree–Fock exchange into the gradient-corrected PBE exchange and correlation functional²⁹ and yields reliable thermochemistry data for reactions involving transition-metal complexes.³⁰ All structures were calculated without geometrical constraints, and all stationary points were characterized as minima or transition states by frequency calculations (i.e., only one negative

frequency for a transition state, no negative frequencies for minima). Solvent effects (*n*-pentane and benzene) were included in all structure optimization and frequency calculations using the PCM implicit solvation model of Tomasi et al. as implemented in the Gaussian code.³¹ No explicit solvent modeling was required because of the extremely low coordinating properties of the hydrocarbon solvents involved in the modeled reactions. Since all tungsten complexes investigated were diamagnetic, all corresponding structures were consequently optimized in the singlet spin state. All charges were computed using an NBO partition analysis.³² Moreover, connections between intermediates and several key transition states were checked using the IRC algorithm.³³

■ ASSOCIATED CONTENT

Supporting Information

The Supporting Information is available free of charge on the ACS Publications website at DOI: 10.1021/acs.organomet.5b00537.

X-ray crystallographic data for complex **11** and NMR spectra of all synthesized unsymmetrical ketones (PDF) Final thermochemical parameters of the various organometallic complexes subjected to DFT calculations (XYZ) Crystallographic data for **11** (CIF)

■ AUTHOR INFORMATION

Corresponding Author

*E-mail for P.L.: legzdins@chem.ubc.ca.

Notes

The authors declare no competing financial interest.

■ ACKNOWLEDGMENTS

We are grateful to The Dow Chemical Company for continuing financial support of our work under Agreement Number 227046 and to our Dow colleagues, Andy Arthur, Brian Kolthammer, Billy Bardin, Devon Rosenfeld, and Brandon Rodriguez, for assistance and helpful discussions. We also thank Travis Nagle for his contribution during the early stages of these investigations. R.A.B. acknowledges the NSERC of Canada for an award of a PGSD postgraduate fellowship. This research has been enabled by the use of WestGrid computing resources, which are funded in part by the Canada Foundation for Innovation, Alberta Innovation, Science BC Advanced Education, and the participating research institutions. WestGrid equipment is provided by IBM, Hewlett-Packard, and SGI.

■ REFERENCES

(1) (a) *Acc. Chem. Res.* **2012**, *45* (6), special issue on CH functionalization. (b) Yamaguchi, J.; Yamaguchi, A. D.; Itami, K. *Angew. Chem., Int. Ed.* **2012**, *51*, 8960–9009. (c) *Chem. Soc. Rev.* **2011**, *40* (4), special issue on C–H functionalization in organic synthesis. (d) *Chem. Rev.* **2010**, *110* (2), special issue on selective functionalization of C–H bonds.
(2) Baillie, R. A.; Legzdins, P. *Acc. Chem. Res.* **2014**, *47*, 330–340.
(3) Baillie, R. A.; Holmes, A. S.; Lefèvre, G. P.; Patrick, B. O.; Shree, M. V.; Wakeham, R. J.; Legzdins, P.; Rosenfeld, D. C. *Inorg. Chem.* **2015**, *54*, 5915–5929.
(4) For synthetically useful reactions employing C–H bond activations for the construction of new C–C bonds, see: (a) Ramirez, T. A.; Zhao, B.; Shi, Y. *Chem. Soc. Rev.* **2012**, *41*, 931–942. (b) Shi, L.; Xia, W. *Chem. Soc. Rev.* **2012**, *41*, 7687–7697. (c) Lewis, J. C.; Bergman, R. G.; Ellman, J. A. *Acc. Chem. Res.* **2008**, *41*, 1013–1025.
(5) Dryden, N. H.; Legzdins, P.; Batchelor, R. J.; Einstein, F. W. B. *Organometallics* **1991**, *10*, 2077–2081.

(6) Baillie, R. A.; Tran, T.; Thibault, M. E.; Legzdins, P. *J. Am. Chem. Soc.* **2010**, *132*, 15160–15161.

(7) See, for example: (a) Cho, C. S. *J. Mol. Catal. A* **2005**, *240*, 55–60. (b) Fujita, K.; Asai, C.; Yamaguchi, T.; Hanasaka, F.; Yamaguchi, R. *Org. Lett.* **2005**, *7*, 4017–4019. (c) Cho, C. S. *Catal. Commun.* **2006**, *7*, 1012–1014.

(8) Palladium-catalyzed reactions: (a) Brunet, J.-J.; Chauvin, R. *Chem. Soc. Rev.* **1995**, *24*, 89–95. (b) Tamaru, Y.; Kimura, M.; Reactions of Acylpalladium Derivatives with Organometals and Related Carbon Nucleophiles. In *Handbook for Organopalladium Chemistry for Organic Synthesis*; Negishi, E.-I., Ed.; Wiley-Interscience: New York, 2002; pp 2425–2454. (c) Hartwig, J. F. *Organotransition Metal Chemistry: From Bonding to Catalysis*; University Science Books: Sausalito, CA, 2010; Chapter 19.

(9) Dieter, R. K. *Tetrahedron* **1999**, *55*, 4177–4236.

(10) Arisawa, M.; Kuwajima, M.; Toriyama, F.; Li, G.; Yamaguchi, M. *Org. Lett.* **2012**, *14*, 3804–3807.

(11) Armarego, W. L. F.; Chai, C. L. L. *Purification of Laboratory Chemicals*, 5th ed.; Elsevier: Amsterdam, 2003.

(12) Compound **5** has been previously reported; see: Ding, B.; Zhang, Z.; Liu, Y.; Sugiyama, M.; Imamoto, T.; Zhang, W. *Org. Lett.* **2013**, *15*, 3690–3693.

(13) Compound **6a** has been previously reported; see: Li, L.; Cai, P.; Guo, Q.; Xue, S. *J. Org. Chem.* **2008**, *73*, 3516–3522.

(14) Compound **6b** has been previously reported; see: Miyoshi, T.; Miyakawa, T.; Ueda, M.; Miyata, O. *Angew. Chem., Int. Ed.* **2011**, *50*, 928–931.

(15) Compound **7** has been previously reported; see: Cheon, C. H.; Kanno, O.; Toste, F. D. *J. Am. Chem. Soc.* **2011**, *133*, 13248–13251.

(16) SHELXT: Sheldrick, G. M. *Acta Crystallogr., Sect. A: Found. Crystallogr.* **2008**, *64*, 112–122.

(17) Cromer, D. T.; Waber, J. T. *International Tables for X-ray Crystallography*; Kynoch Press: Birmingham, U.K., 1974; Vol. IV, Table 2.2A.

(18) Ibers, J. A.; Hamilton, W. C. *Acta Crystallogr.* **1964**, *17*, 781–782.

(19) Creagh, D. C.; McAuley, W. J. *International Tables for X-ray Crystallography*; Kluwer Academic: Boston, MA, 1992; Vol. C, Table 4.2.6.8.

(20) Creagh, D. C.; Hubbell, J. H. *International Tables for X-ray Crystallography*; Kluwer Academic: Boston, MA, 1992; Vol. C, Table 4.2.4.3.

(21) SHELXL-2014: Sheldrick, G. M. *Acta Crystallogr., Sect. A: Found. Adv.* **2015**, *71*, 3–8.

(22) OLEX2-V1.2.6: Dolomanov, O. V.; Bourhis, L. J.; Gildea, R. J.; Howard, J. A. K.; Puschmann, H. *J. Appl. Crystallogr.* **2009**, *42*, 339–341.

(23) Parr, R. G.; Yang, W. *Density-Functional Theory of Atoms and Molecules*; Oxford University Press: Oxford, U.K., 1989.

(24) Frisch, M. J., et al. *Gaussian 09, Revision D.01*; Gaussian, Inc., Wallingford, CT, 2013.

(25) Krishnan, R.; Binkley, J. S.; Seeger, R.; Pople, J. A. *J. Chem. Phys.* **1980**, *72*, 650–654.

(26) Clark, T.; Chandrasekhar, J.; Spitznagel, G. W.; Schleyer, P. v. R. *J. Comput. Chem.* **1983**, *4*, 294–301.

(27) von Szentpály, L.; Fuentealba, P.; Preuss, H.; Stoll, H. *Chem. Phys. Lett.* **1982**, *93*, 555–559.

(28) Adamo, C.; Barone, V. *J. Chem. Phys.* **1999**, *110*, 6158–6169.

(29) Perdew, J. P.; Burke, K.; Ernzerhof, M. *Phys. Rev. Lett.* **1996**, *77*, 3865–3868.

(30) Coquet, R.; Tada, M.; Iwasawa, Y. *Phys. Chem. Chem. Phys.* **2007**, *9*, 6040–6046.

(31) (a) Miertuš, S.; Scrocco, E.; Tomasi, J. *Chem. Phys.* **1981**, *55*, 117–129. (b) Scalmani, G.; Frisch, M. J.; Mennucci, B.; Tomasi, J.; Cammi, R.; Barone, V. *J. Chem. Phys.* **2006**, *124*, 094107.

(32) Foster, J. P.; Weinhold, F. *J. Am. Chem. Soc.* **1980**, *102*, 7211–7218.

(33) Hratchian, H. P.; Schlegel, H. B. *J. Chem. Phys.* **2004**, *120*, 9918–9924.